Intestinal Inflammation Targets Cancer-Inducing Activity of the Microbiota

Janelle C. Arthur *et al.*

Science **338**, 120 (2012);
DOI: 10.1126/science.1224820

Science (print ISSN 0036-8075; online ISSN 1095-9203) is published weekly, except the last week in December, by the American Association for the Advancement of Science, 1200 New York Avenue NW, Washington, DC 20005.

Intestinal Inflammation Targets Cancer-Inducing Activity of the Microbiota

Janelle C. Arthur,[1] Ernesto Perez-Chanona,[1] Marcus Mühlbauer,[1] Sarah Tomkovich,[1] Joshua M. Uronis,[1] Ting-Jia Fan,[1] Barry J. Campbell,[2] Turki Abujamel,[3,4] Belgin Dogan,[5] Arlin B. Rogers,[6] Jonathan M. Rhodes,[2] Alain Stintzi,[3] Kenneth W. Simpson,[5] Jonathan J. Hansen,[1] Temitope O. Keku,[1] Anthony A. Fodor,[7] Christian Jobin[1]*

Inflammation alters host physiology to promote cancer, as seen in colitis-associated colorectal cancer (CRC). Here, we identify the intestinal microbiota as a target of inflammation that affects the progression of CRC. High-throughput sequencing revealed that inflammation modifies gut microbial composition in colitis-susceptible interleukin-10–deficient (*Il10*$^{-/-}$) mice. Monocolonization with the commensal *Escherichia coli* NC101 promoted invasive carcinoma in azoxymethane (AOM)–treated *Il10*$^{-/-}$ mice. Deletion of the polyketide synthase (*pks*) genotoxic island from *E. coli* NC101 decreased tumor multiplicity and invasion in AOM/*Il10*$^{-/-}$ mice, without altering intestinal inflammation. Mucosa-associated *pks*$^{+}$ *E. coli* were found in a significantly high percentage of inflammatory bowel disease and CRC patients. This suggests that in mice, colitis can promote tumorigenesis by altering microbial composition and inducing the expansion of microorganisms with genotoxic capabilities.

Chronic inflammation is a well-established risk factor for several cancers, including colorectal cancer (CRC) (*1*). Although the mechanism by which chronic intestinal inflammation leads to CRC is still unclear, numerous experimental studies suggest that inflammatory cells and their associated mediators such as interleukin-6 (IL-6), tumor necrosis factor–α (TNF-α), IL-23, and reactive oxygen species form a microenvironment favoring the development of CRC, presumably by enhancing DNA damage in epithelial cells (*2*–*4*).

In the colon, trillions of commensal bacteria, termed "the microbiota," are in close proximity to a single layer of epithelial cells. A critical question is whether these microorganisms actively participate in the process of carcinogenesis. We have previously shown that microbial status modulates development of colitis-associated CRC by using the colitis-susceptible *Il10*$^{-/-}$ mouse strain (*5*). To evaluate the effect of inflammation and carcinogenesis on the colonic microbiota, we used Illumina (San Diego, California) HiSeq. 2000 sequencing targeting the hypervariable V6 region of the 16*S* ribosomal RNA (rRNA) gene in mucosal biopsies and stool samples of *Il10*$^{-/-}$ and wild-type (WT) mice, in the presence and absence of the colon-specific carcinogen azoxymethane (AOM). Germ-free (GF) *Il10*$^{-/-}$ and control WT adult mice were transferred to specific pathogen–free (SPF) conditions for 20 weeks. During this time frame, 100% of *Il10*$^{-/-}$ mice develop colitis; with the addition of AOM, 60 to 80% of mice develop colon tumors (*5*). WT mice developed neither colitis nor tumors (*5*). We first compared the luminal microbiota between all *Il10*$^{-/-}$ (colitis/cancer) and WT mice (healthy control) and found that the microbiota of *Il10*$^{-/-}$ mice clustered apart from those of WT controls [analysis of similarity (ANOSIM) $R = 0.925$, $P = 0.002$] (Fig. 1A and fig. S1). The altered microbiota of *Il10*$^{-/-}$ mice showed reduced richness as compared with that of WT controls ($P < 0.0001$) (Fig. 1B). Analysis of mucosal biopsies revealed the colonic-adherent microbiota of AOM/*Il10*$^{-/-}$ mice with colitis/cancer clustered apart from healthy AOM/WT controls (fig. S2A), with alterations in microbial evenness but not richness ($P = 0.023$) (fig. S2B). To determine the impact of AOM on the microbiota in the context of inflammation, we compared the luminal microbiota of *Il10*$^{-/-}$ mice with colitis with that of AOM/*Il10*$^{-/-}$ mice with colitis/cancer and found that AOM treatment had no significant effect on luminal microbial composition or richness in *Il10*$^{-/-}$ mice (Fig. 1, C and D). These data suggest that inflammation rather than cancer is associated with the observed microbial shifts.

We then hypothesized that inflammation-induced changes in microbial composition include the expansion of bacteria within the Proteobacteria phylum because several members have been associated with colitis and CRC (*6*–*9*). Analysis of phylum-level distribution revealed that inflammation in *Il10*$^{-/-}$ mice was associated with significantly increased levels of luminal Verrucomicrobia, Bacteroidetes, and Proteobacteria as compared with that of WT controls (fig. S3). Although Verrucomicrobia significantly differed between groups, this phylum is not well characterized, restricting detailed molecular analysis. Within Proteobacteria, however, the Gammaproteobacteria class, Enterobacteriales order, and Enterobacteriaceae family were all significantly more abundant in *Il10*$^{-/-}$ mice (Fig. 1, E to H). Because *E. coli* are members of the family Enterobacteriaceae and adherent-invasive *E. coli* have been associated with human inflammatory bowel disease (IBD) and CRC (*8*, *10*–*13*), we determined by means of quantitative polymerase chain reaction (PCR) whether *E. coli* was more abundant in the context of inflammation in *Il10*$^{-/-}$ mice. We found that relative to WT mice, the luminal microbiota of *Il10*$^{-/-}$ mice exhibited a ~100-fold increase in *E. coli* (Fig. 1I). AOM treatment did not affect *E. coli* abundance (fig. S4A). Total bacterial loads between WT and *Il10*$^{-/-}$ mice did not differ (fig. S4B), nor did levels of the common commensal *Lactobacillus* (fig. S4C).

To determine the causative effect of commensal *E. coli* on CRC, we administered AOM to GF *Il10*$^{-/-}$ mice mono-associated with either the commensal mouse adherent-invasive *E. coli* NC101 or the human commensal *Enterococcus faecalis* OG1RF, both of which cause aggressive colitis in *Il10*$^{-/-}$ mice (*14*). As expected, both *E. coli* NC101 and *E. faecalis* mono-associated, AOM-treated *Il10*$^{-/-}$ mice developed severe colitis (Fig. 2A). Despite similar levels of colitis, 80% of *E. coli* mono-associated mice developed invasive mucinous adenocarcinoma, whereas *E. faecalis* mono-associated mice rarely developed tumors (Fig. 2, B to D). Colonic cytokines involved in inflammation and carcinogenesis including *Il6*, *Tnfa*, *Ifng*, *Il1b*, *Il18*, *Il17*, *and Il23* were not significantly different between AOM-treated *E. coli* and *E. faecalis* mono-associated mice (Fig. 2E, fig. S5, and tables S1 and S2). In addition, infiltrating CD3^{+} T cells, F4/80^{+} macrophages, and Ly6B.2^{+} monocytes and neutrophils were similar between AOM-treated *E. coli* and *E. faecalis* mono-associated mice (fig. S6). These observations demonstrate that in addition to inflammation, bacteria-specific factors may be required for the development of colitis-associated CRC.

We hypothesized that *E. coli* NC101 has carcinogenic capabilities not shared by *E. faecalis.* Several members of the family *Enterobacteriaceae*, including select *E. coli* strains of B2 phylotype, harbor a ~54-kb *polyketide synthases* (*pks*) pathogenicity island that encodes multi-enzymatic machinery for synthesizing a peptide-polyketide hybrid genotoxin named Colibactin (*15*–*18*). A bioinformatics Basic Local Alignment Search Tool (BLAST) search of the *E. coli* NC101 genome (accession NZ_AEFA00000000) revealed the presence of *pks* and the absence of other known

[1]Department of Medicine, Pharmacology and Immunology-Microbiology, University of North Carolina at Chapel Hill, Chapel Hill, NC 27599, USA. [2]Department of Gastroenterology, University of Liverpool, Liverpool L69 3BX, UK. [3]Ottawa Institute of Systems Biology, Department of Biochemistry, Microbiology and Immunology, Faculty of Medicine, University of Ottawa, Ontario K1H 8M5, Canada. [4]Department of Medical Technology, Faculty of Applied Medical Sciences, King Abdulaziz University, Jeddah 21589, Saudi Arabia. [5]Department of Clinical Sciences, Cornell University, Ithaca, NY 14853, USA. [6]Lineberger Comprehensive Cancer Center, Department of Pathology and Laboratory Medicine, University of North Carolina at Chapel Hill, Chapel Hill, NC 27599, USA. [7]Department of Bioinformatics and Genomics, University of North Carolina at Charlotte, Charlotte, NC 28223, USA.

*To whom correspondence should be addressed. E-mail: job@med.unc.edu

E. coli genotoxins Cif, CNF, and CDT. Using PCR and sequencing (*15*), we detected the *pks* island in *E. coli* NC101 but not in *E. faecalis* or non-colitogenic *E. coli* K12 (Fig. 3A). To determine whether *E. coli pks* is associated with human CRC or IBD, we screened mucosa-associated *E. coli* strains isolated from colorectal tissue specimens of 35 patients with IBD, 21 with CRC, and 24 non-IBD/non-CRC controls (*11*). CRC specimens could not be obtained from IBD-associated CRC patients because these patients typically undergo colectomy upon diagnosis of dysplasia. Although 5 of the 24 (20.8%) non-IBD/non-CRC controls harbored *pks*$^+$ *E. coli*, the genotoxic island was detected in 14 of 35 (40%, $P < 0.05$) IBD patients and in 14 of 21 (66.7%, $P < 0.001$) CRC patients (Fig. 3B and table S3). This suggests that *pks*$^+$ bacteria are associated with chronic intestinal inflammation and CRC and may affect carcinogenesis.

To functionally link *pks* with the development of CRC, we created an isogenic *pks*-deficient *E. coli* NC101 strain (NC101Δ*pks*). Absence of *pks* did not affect bacterial growth in vitro (fig. S7), nor did it impair colonization capacity in vivo (10^9 to 10^{10} per 200 g stool pellet, four to six mice per group). Because *pks* from strains of extraintestinal pathogenic *E. coli* can elicit mammalian DNA damage (*15*, *16*), we tested the ability of *E. coli* NC101 *pks* to induce a DNA damage response. We infected the nontransformed rat intestinal epithelial cell line IEC-6 with NC101 or NC101Δ*pks* and assessed levels of phosphorylated histone H2AX (γH2AX), which is a surrogate marker of DNA damage (*19*–*21*). WT NC101 induced γH2AX in ~30% of cells, whereas NC101Δ*pks* induced γH2AX in <5%, which is a level equivalent to that induced by non-colitogenic *E. coli* K12 (Fig. 3C). Consistent with these results, we observed that WT NC101 induced a threefold increase in the percent of cells arrested in G_2/M phase relative to untreated and NC101Δ*pks*-infected cells (Fig. 3D). These experiments demonstrate that *pks* alone has the capacity to induce DNA damage and indicate that the genotoxic island does not block the initiation of DNA damage response. This led us to hypothesize that *pks* would also promote tumorigenesis in vivo.

To test this hypothesis, we mono-associated GF *Il10*$^{-/-}$ mice with *E. coli* NC101 or NC101Δ*pks*, with or without AOM treatment, and assessed inflammation and tumorigenesis. The absence of *pks* did not affect the severity of colonic inflammation in *Il10*$^{-/-}$ mice with colitis (12 weeks with no AOM), or colitis/cancer (14 and 18 weeks with AOM) (Fig. 4A). Similarly, colon tissue pro-inflammatory cytokine transcripts and immune cell infiltration were not significantly different between mice mono-associated with NC101 versus NC101Δ*pks* (figs. S8 and S9 and table S4). However, at both 14 and 18 weeks with AOM, the absence of *pks* was associated with significantly reduced neoplastic lesions (Fig. 4B). At 14 weeks with AOM, high-grade dysplasia (HGD) or invasive carcinomas were present in five of eight mice mono-associated with NC101, whereas only one of eight NC101Δ*pks* mono-associated mice developed HGD. At 18 weeks with AOM, the absence of *pks* did not affect mouse survival or tumor size; however, macroscopic tumor burden and carcinoma invasion were significantly decreased (Fig. 4, C to F, and fig. S10). In addition, all nine NC101 mono-associated mice developed invasive carcinoma, with four of nine fully invading the muscularis propria and serosa. In contrast, zero of nine NC101Δ*pks* mono-associated mice exhibited full invasion. This likely suggests that the presence of *E. coli pks* accelerates progression from dysplasia to invasive carcinoma. In the absence of AOM, GF *Il10*$^{-/-}$ mice colonized with NC101 for 21 weeks developed only mild dysplasia (fig. S11A). GF WT mice mono-associated with *E. coli* NC101 and treated with AOM developed neither inflammation nor dysplasia/tumors (fig. S11B), suggesting that this bacterium is not carcinogenic in the absence of inflammation. Together, these data indicate that the absence of *pks* reduces the tumorigenic potential of *E. coli* NC101 without altering colonic inflammation.

To evaluate the impact of *pks* on host DNA damage in vivo, we measured colonocyte γH2AX$^+$ nuclear foci (γ-foci) in AOM/*Il10*$^{-/-}$ mice mono-associated with NC101 versus NC101Δ*pks* for 14 weeks (*19*–*21*). The abundance of γ-foci$^+$ colonocytes/crypt was significantly reduced in AOM/*Il10*$^{-/-}$ mice mono-associated with *E. coli* NC101Δ*pks* versus *E. coli* NC101 (Fig. 4G). We detected an 80% reduction in γ-foci$^+$ colonocytes/crypt in *E. coli* NC101 mono-associated AOM/WT mice relative to *E. coli* NC101-associated AOM/*Il10*$^{-/-}$ mice (Fig. 4G). This suggests that both host inflammation and *E. coli*–derived *pks* act in concert to create a host microenvironment that promotes DNA damage and tumorigenesis in AOM/*Il10*$^{-/-}$ mice.

Although the etiology of colitis-associated CRC is multifactorial, this work indicates that chronic inflammation targets the intestinal microbiota and can induce the expansion of microbes, including *E. coli*, that influence CRC in mice. The

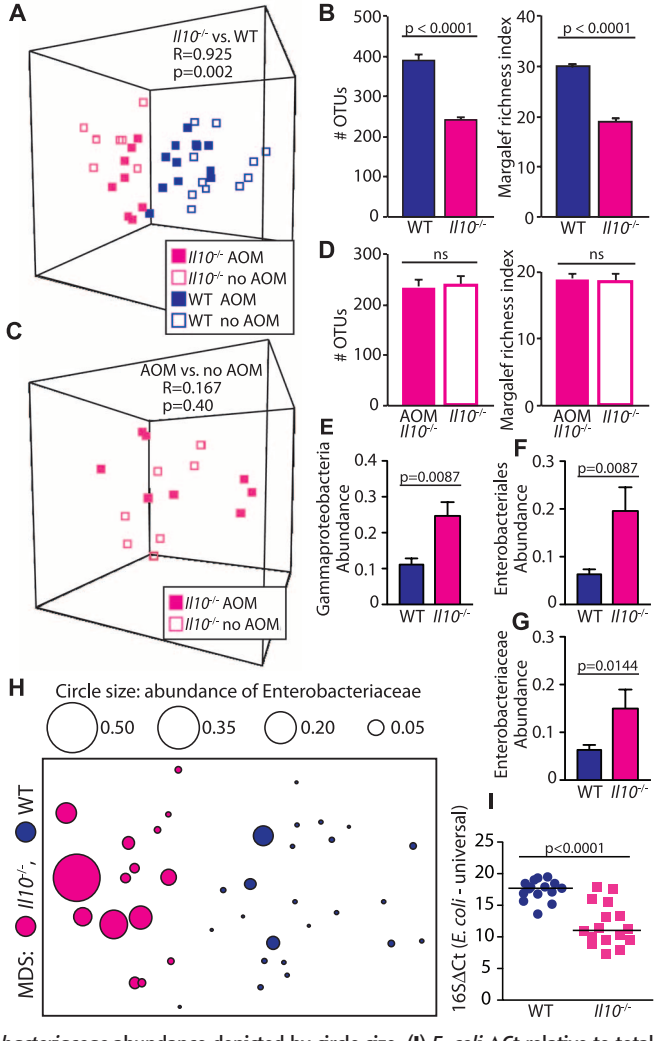

Fig. 1. Inflammation alters fecal microbial community structure. (**A** and **B**) Luminal microbiota of *Il10*$^{-/-}$ versus WT mice. (A) Operational taxonomic unit (OTU) abundances were standardized by total, square root transformed, and assembled into a Bray Curtis similarity matrix to generate a multidimensional scaling (MDS) plot, where in these plots each symbol represents the microbiota of an individual mouse analyzed by means of Illumina sequencing of 16*S* V6 region. *Il10*$^{-/-}$ versus WT comparison is by ANOSIM, $R = 1$ is maximum dissimilarity. (B) Richness, mean + SEM of cage means, five to six cages per group, two to four mice per cage, *t* test. (**C** and **D**) Luminal microbiota of AOM/*Il10*$^{-/-}$ versus *Il10*$^{-/-}$ (C) MDS plot, AOM/*Il10*$^{-/-}$ versus *Il10*$^{-/-}$ comparison by ANOSIM. (D) Richness, mean + SEM of cage means, two to three cages per group, two to four mice per cage, *t* test. (**E** to **G**) Standardized transformed abundance, median + SEM of cage means, five to six cages per group, two to four mice per cage, Mann Whitney *U* test. (**H**) MDS plot depicting luminal microbiota of *Il10*$^{-/-}$ versus WT, overlaid with *Enterobacteriaceae* abundance depicted by circle size. (**I**) *E. coli* ΔCt relative to total bacteria (16*S*). Each symbol depicts one mouse, line at median, Mann Whitney *U* test.

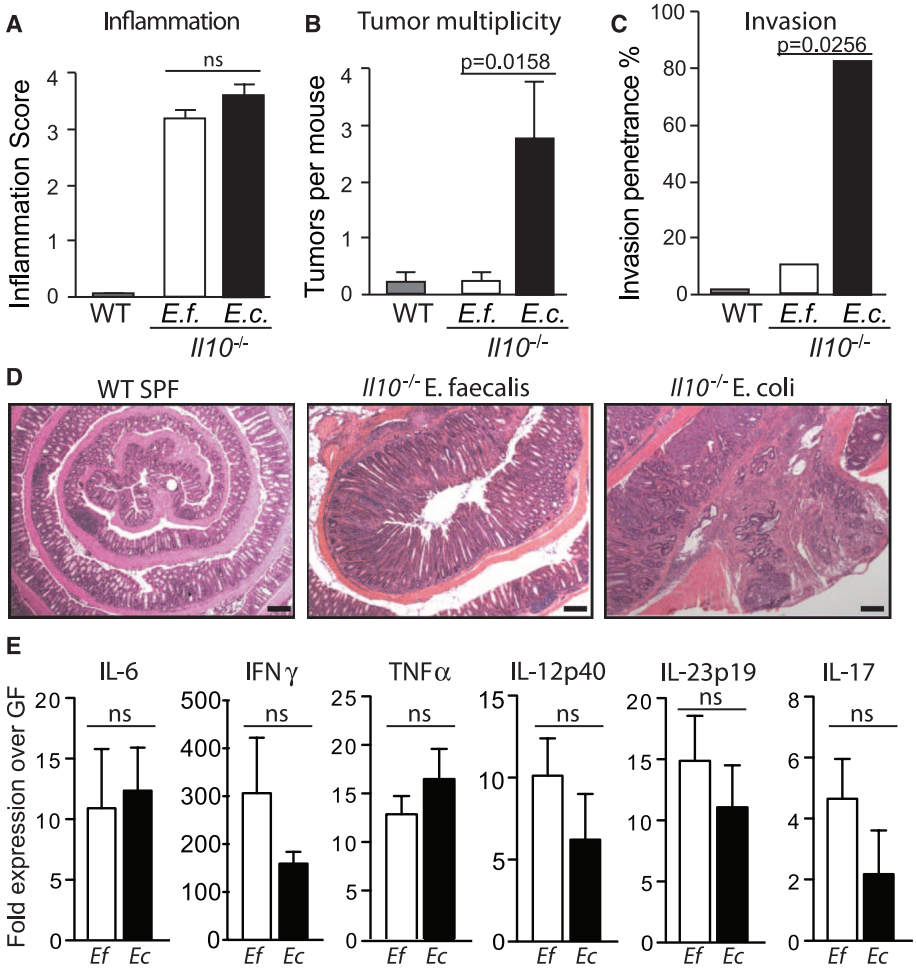

Fig. 2. Colonization of germ-free mice *Il10*$^{-/-}$ mice with *E. coli* (*E.c.*) or *E. faecalis* (*E.f.*) differentially affects tumorigenesis without affecting inflammation. (**A**) Histologic inflammation scores, *t* test. (**B**) Macroscopic tumor counts; two-tailed Mann Whitney *U* rank sum test. (**C**) Percent of mice with invasive adenocarcinoma; Fisher's exact test. (**D**) Representative hematoxylin and eosin (H&E) histology. In (A) to (D), mean + SEM, 7 to 12 per group, single experiment. (**E**) Colonic cytokine mRNA expression relative to GF *Il10*$^{-/-}$; mean + SEM, four samples per group, *t* test.

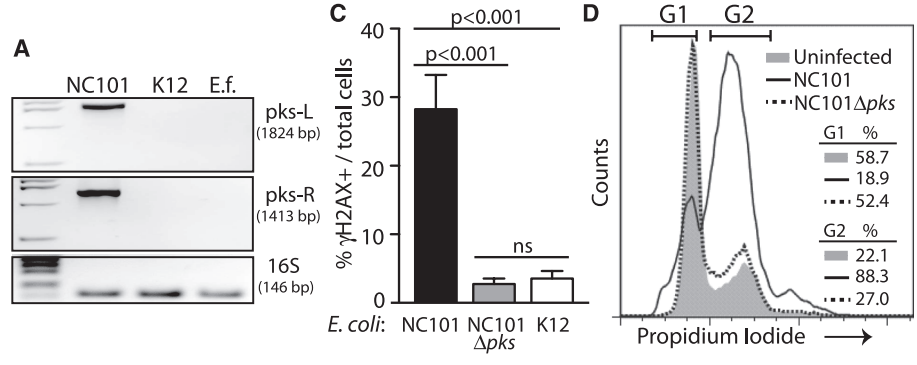

Fig. 3. *pks*$^{+}$ *E. coli* strains are associated with CRC and DNA damage. (**A** and **B**) PCR screen for *pks* (A) using primers targeting the left [1824 base pair (bp)] and right (1413 bp) ends of the *pks* island in *E. coli* strains NC101 and K12, and *E. faecalis* (E.f.), and (B) using primers targeting the right end and *ClbB* gene of the *pks* island in mucosa-associated *E. coli* isolated from human colorectal tissue specimens. Binomial test **P* < 0.05, ****P* < 0.001. (**C** and **D**) NC101 *pks* induces (C) γH2AX (MOI 20, 4 hours) in IEC-6 cells; mean + SEM, analysis of variance (ANOVA) + Tukey, and (D) G2 cell cycle arrest (MOI 100, 24 hours). (A), (C), and (D) are representative of three experiments.

B

Disease	# Patients[1]	ClbB+	Pks+	% ClbB+Pks+	*p* value[2]
CRC	21	15	14	66.7	*p<0.001*
IBD	35	14	14	40.0	*p<0.05*
Control[3]	24	5	5	20.8	

[1] *Mucosa-associated E. coli was isolated from colon tissue specimens*
[2] *Differences in # ClbB+Pks+ patients vs controls were assessed using the binomial test*
[3] *Control = non-CRC, non-IBD patients (see Table S3)*

carcinogenic effect of *E. coli* NC101 *pks* clearly demonstrates that genotoxic microorganisms promote CRC in the presence of the carcinogen AOM in *Il10*$^{-/-}$ mice. It remains to be seen whether NC101 and other *pks*-harboring bacteria have similar effects in other models of colitis-associated CRC. An increased prevalence of *pks*$^{+}$ *E. coli* in IBD and CRC patients may suggest a cancer-promoting role in human CRC. We propose a model in which inflammation creates an environment that supports carcinogenesis through its effects on both the host and the microbiota. In

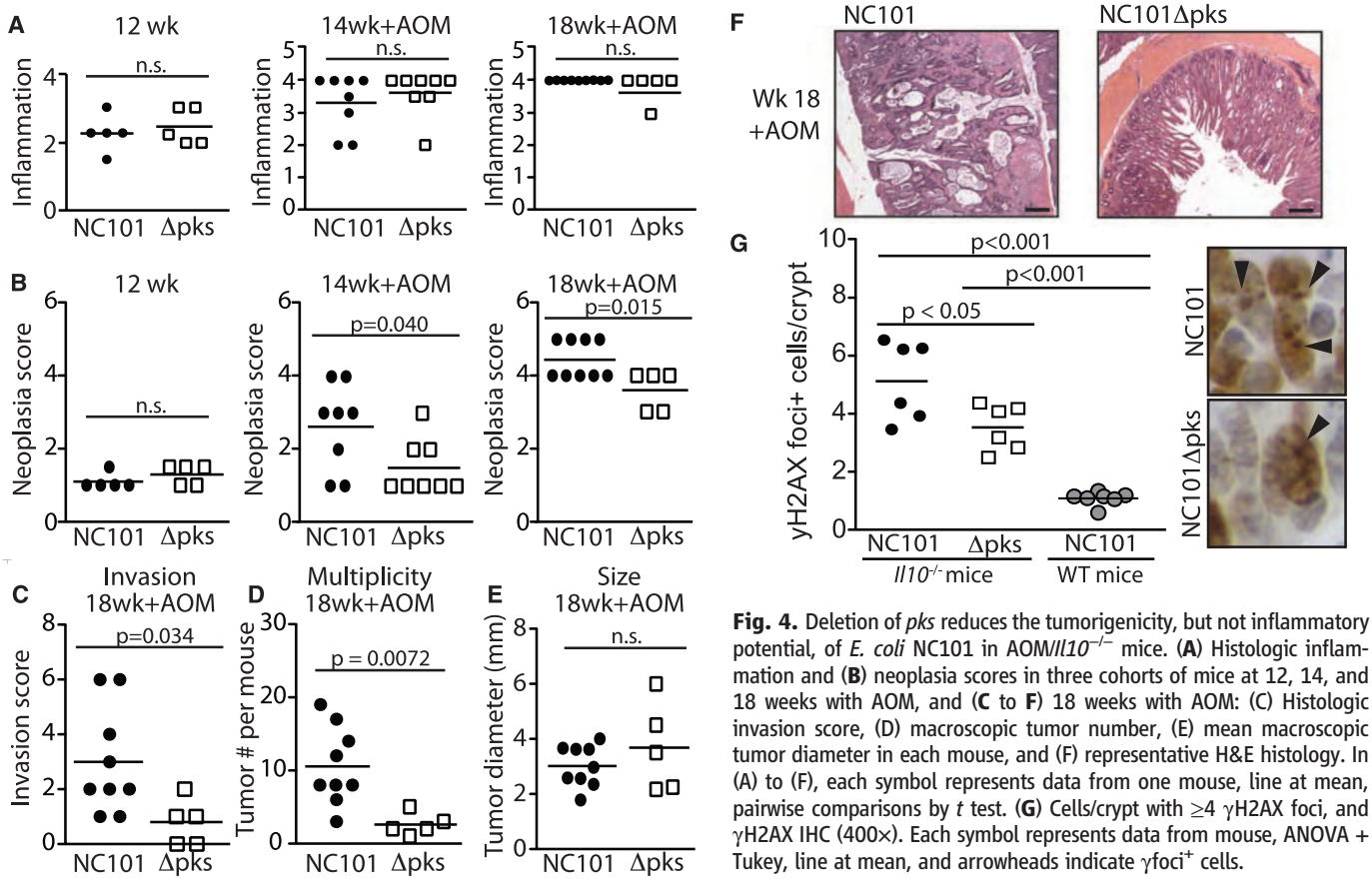

Fig. 4. Deletion of *pks* reduces the tumorigenicity, but not inflammatory potential, of *E. coli* NC101 in AOM/*Il10*$^{-/-}$ mice. (**A**) Histologic inflammation and (**B**) neoplasia scores in three cohorts of mice at 12, 14, and 18 weeks with AOM, and (**C** to **F**) 18 weeks with AOM: (C) Histologic invasion score, (D) macroscopic tumor number, (E) mean macroscopic tumor diameter in each mouse, and (F) representative H&E histology. In (A) to (F), each symbol represents data from one mouse, line at mean, pairwise comparisons by *t* test. (**G**) Cells/crypt with ≥4 γH2AX foci, and γH2AX IHC (400×). Each symbol represents data from mouse, ANOVA + Tukey, line at mean, and arrowheads indicate γfoci^{+} cells.

this two-hit model, inflammation targets the microbiota to foster the expansion of bacteria with genotoxic potential, such as *pks*$^{+}$ bacteria. In parallel, inflammation creates an opportunity for *pks*$^{+}$ bacteria to adhere to the colonic mucosa by decreasing protective mucins and antimicrobial peptide production (*22*–*24*)—a process prevented by natural barrier function present in noninflamed WT mice. The genotoxic effect of *pks* requires bacteria-host cell contact (*15*, *16*); thus, an environment in which bacteria can more readily access the epithelium could result in increased delivery of the *pks* product Colibactin to epithelial host cells. This would explain the lack of cancer in *pks*$^{+}$ *E. coli*–associated WT mice. Although other microbes likely participate in the progression of CRC, our findings highlight the complex effects of inflammation on both microbial composition/activity and the host's ability to protect itself from a dysbiotic microbiota (*25*).

References and Notes

1. F. Balkwill, A. Mantovani, *Lancet* **357**, 539 (2001).
2. T. A. Ullman, S. H. Itzkowitz, *Gastroenterology* **140**, 1807 (2011).
3. W.-W. Lin, M. Karin, *J. Clin. Invest.* **117**, 1175 (2007).
4. S. Danese, A. Mantovani, *Oncogene* **29**, 3313 (2010).
5. J. M. Uronis *et al.*, *PLoS ONE* **4**, e6026 (2009).
6. W. S. Garrett *et al.*, *Cell Host Microbe* **8**, 292 (2010).
7. S. A. Luperchio, D. B. Schauer, *Microbes Infect.* **3**, 333 (2001).
8. X. J. Shen *et al.*, *Gut Microbes* **1**, 138 (2010).
9. B. J. Marshall, *JAMA* **274**, 1064 (1995).
10. A. Swidsinski *et al.*, *Gastroenterology* **115**, 281 (1998).
11. H. M. Martin *et al.*, *Gastroenterology* **127**, 80 (2004).
12. A. Darfeuille-Michaud *et al.*, *Gastroenterology* **115**, 1405 (1998).
13. E. Masseret *et al.*, *Gut* **48**, 320 (2001).
14. S. C. Kim *et al.*, *Gastroenterology* **128**, 891 (2005).
15. J. P. Nougayrède *et al.*, *Science* **313**, 848 (2006).
16. G. Cuevas-Ramos *et al.*, *Proc. Natl. Acad. Sci. U.S.A.* **107**, 11537 (2010).
17. S. Homburg, E. Oswald, J. Hacker, U. Dobrindt, *FEMS Microbiol. Lett.* **275**, 255 (2007).
18. J. Putze *et al.*, *Infect. Immun.* **77**, 4696 (2009).
19. E. P. Rogakou, D. R. Pilch, A. H. Orr, V. S. Ivanova, W. M. Bonner, *J. Biol. Chem.* **273**, 5858 (1998).
20. E. P. Rogakou, C. Boon, C. Redon, W. M. Bonner, *J. Cell Biol.* **146**, 905 (1999).
21. K. Rothkamm, M. Löbrich, *Proc. Natl. Acad. Sci. U.S.A.* **100**, 5057 (2003).
22. Y. Inaba *et al.*, *Inflamm. Bowel Dis.* **16**, 1488 (2010).
23. N. M. J. Schwerbrock *et al.*, *Inflamm. Bowel Dis.* **10**, 811 (2004).
24. J. M. Rhodes, B. J. Campbell, *Trends Mol. Med.* **8**, 10 (2002).
25. Materials and methods are available as supplementary materials on *Science* Online.

Acknowledgments: We thank M. Bower and S. Tonkonogy of the National Gnotobiotic Rodent Resource Center at University of North Carolina (UNC) and North Carolina State University for assistance with gnotobiotic mice (NIH P40 R018603). Histology was performed at the Center for Gastrointestinal Biology and Diseases histology core (P30 DK034987). This work was supported by funding from NIH T32 DK007737 (J.C.A.), R01 DK73338 (C.J.), R01 DK47700 (C.J.), R01 CA136887 (T.O.K.), R01 DK53347-11 (K.W.S./A.B.S.), the American Institute for Cancer Research (C.J.), UNC University Cancer Research Fund (C.J.), New York Presbyterian/Weill Cornell Medical College (K.W.S.), Crohn's and Colitis foundation UK (B.J.C.), the NIH Research Specialist Biomedical Research Center in Microbial Disease (J.M.R.), the North West Cancer Research Fund UK (B.J.C.), and the Canadian Institutes of Health Research MOP#114872 (A.S.). T.A. is supported by a scholarship from King Abdulaziz University, through the Saudi Arabian Cultural Bureau in Canada. J.M.R. is a member of advisory boards for Atlantic, Procter and Gamble, and Falk and has received speaking honoraria from Abbott, Falk, Ferring, GlaxoSmithKline, Procter and Gamble, Schering Plough, Shire, and Wyeth. All data presented in this manuscript are tabulated in the main paper and in the supplementary materials. Illumina sequencing data are deposited in National Center for Biotechnology Information's (NCBI's) sequence read archive (SRA) and are accessible under SRA055272. Inflammation PCR array data are deposited in NCBI's Gene Expression Omnibus (GEO) and are accessible through GEO series accession no. GSE39085. This work is in the memory of Mathieu Jobin, Lyne Gauthier, and Janine Drysdale.

Supplementary Materials

www.sciencemag.org/cgi/content/full/science.1224820/DC1
Materials and Methods
Figs. S1 to S11
Tables S1 to S4
References (*26*–*39*)

17 May 2012; accepted 1 August 2012
Published online 16 August 2012;
10.1126/science.1224820